PB-220 480

IMPROVEMENT OF OPTICAL EFFICIENCY OF LUMINESCENCE OF A FLAME PHOTOMETRIC DETECTOR

Baird-Atomic, Incorporated

Prepared for:

Environmental Protection Agency

December 1972

DISTRIBUTED BY:

NTIS

National Technical Information Service
U. S. DEPARTMENT OF COMMERCE
5285 Port Royal Road, Springfield Va. 22151

EPA-R2-73-193

PB 220 480

Reproduced by
NATIONAL TECHNICAL
INFORMATION SERVICE
U S Department of Commerce
Springfield VA 22151

BIBLIOGRAPHIC DATA SHEET	1. Report No. EPA-R2-73-193	2.	3. Recipient's Accession No. PB-220 480
4. Title and Subtitle: Improvement of Optical Efficiency of Luminescence of a Flame Photometric Detector			5. Report Date: December 1972 6.
7. Author(s)			8. Performing Organization Rept. No.
9. Performing Organization Name and Address: Baird-Atomic, Inc. 125 Middlesex Turnpike Bedford, Massachusetts 01730			10. Project/Task/Work Unit No. 11. Contract/Grant No. EHSD 71-50
12. Sponsoring Organization Name and Address: ENVIRONMENTAL PROTECTION AGENCY Research Triangle Park, North Carolina 27711			13. Type of Report & Period Covered: Final 14.

15. Supplementary Notes

16. Abstracts

A project was initiated with principal objective being to increase the optical efficiency of the Melpar flame photometric detector for the detection of SO_2. Two routes were explored. First, the spatial distribution of sulfur and background emissions were plotted to establish regions of greatest signal/background. Second, multi-slits were constructed to match the structured sulfur emission and allow background substract. The spatial studies of sulfur and background emission demonstrated that the optimum signal/background is obtained below the geometric center of the standard burner. The distribution suggested use of a monochromator with horizontal entrance slit rather than a filter. A study of the line emission of sulfur demonstrated that multiple slits could be constructed which would both increase specificity for sulfur and increase the usable signal. Using multi-slits in the non-differential mode the final sensitivity was about an order of magnitude greater than the comparison standard instrument.

17. Key Words and Document Analysis. 17a. Descriptors

Air pollution
Sulfur dioxide
Optical activity
Efficiency
Optical detection
Flame photometry
Emission
Instruments
Operations

17b. Identifiers/Open-Ended Terms

Air pollution detection

17c. COSATI Field/Group 13B

18. Availability Statement	19. Security Class (This Report)	21. No. of Pages
Unlimited	UNCLASSIFIED	~~41~~ 42
	20. Security Class (This Page) UNCLASSIFIED	22. Price $3.00 / 1.45

IMPROVEMENT OF OPTICAL EFFICIENCY OF LUMINESCENCE OF A FLAME PHOTOMETRIC DETECTOR

Contract No. EHSD 71-50

Prepared for

Environmental Protection Agency
Research Triangle Park
Durham, North Carolina 27711

December 1972

Final Report

Approved by: A. W. Hornig

Arthur W. Hornig
Director of Research
Government Systems Division

Baird-Atomic, Inc.
125 Middlesex Turnpike
Bedford, Massachusetts 01730

TABLE OF CONTENTS

Section		Page
1.	INTRODUCTION AND SUMMARY	1-1
2.	LABORATORY STUDIES	2-1
2.1	Standard Instrument Evaluation	2-1
2.2	S_2 Emission Studies	2-1
2.3	Background Emission Studies	2-4
2.4	Choice of Monochromator System	2-5
2.5	Multiple Slit Studies	2-6
2.6	Background Subtract Mechanism	2-7
2.7	Electronic Modifications	2-7
2.8	Laboratory Measurements	2-8
2.8.1	Modes of Operation	2-9
2.8.2	Single Slit Mode	2-9
2.8.3	Multi-Slit Mode	2-10
2.8.4	Multi-Slit Differential Mode	2-10
2.9	Instrument Packaging and Controls	2-11
2.9.1	Electronics	2-12
2.9.2	Burner, Monochromator and Photomultiplier Detector	2-12
2.9.3	Quartz Plate Drive Mechanism	2-13
2.10	Delivery Demonstration at Research Triangle Park	2-13
3.	DISCUSSION AND RECOMMENDATIONS	3-1
3.1	Recommendations	3-2
4.	OPERATIONAL PROCEDURES	4-1
4.1	Operating Controls	4-1
4.2	Operation Start-Up	4-1
4.3	Recorder Input	4-1
4.4	Calibration	4-1
4.5	Gas Flow System	4-2
4.6	Maintenance	4-2
4.7	Differential Mode	4-2

LIST OF ILLUSTRATIONS

Figure No.	
1	Vertical Spatial Scan
2	Spatial Distribution of S_2 Emission (Clean Burner)
3	Spatial Distribution of S_2 Emission (Dirty Burner)
4	Spectral Distribution of S_2 Emission with 2 nm Bandwidth
5	Spectral Distribution of S_2 Emission/Background (Burner Center)
6	Spectral Distribution of S_2 Emission at Different Concentrations
7	Spectral Distribution of Flame Background Emission
8	Spatial Distribution of Flame Background (310 nm line)
9	S_2 Spectra at Exit Plane of Monochromator for Different Entrance Slits
10	Amplifier/Demodulator Schematic
11	Spectral Distribution of S_2 Emission with 3.5 nm Bandwidth
12	Spectral Distribution of S_2 Emission with 5 nm Bandwidth
13	Comparison of Multi-Slits and Single Slits
14	SO_2 Monitoring with Multi-Slits in Differential Mode
15	Modified SO_2 Analyzer (Right Side)
16	Modified SO_2 Analyzer (Left Side)
17	Modified SO_2 Analyzer (Top View)

1. INTRODUCTION AND SUMMARY

The principal objective of this contract was to increase the optical efficiency of the Melpar flame photometric detector for the detection of SO_2. Such increased efficiency should lead to higher sensitivity, stability and freedom from interference. Two routes were explored. First, the spatial distribution of sulfur and background emissions were plotted to establish regions of greatest signal/background. Second, multi-slits were constructed to match the structured sulfur emission and allow background subtract. The spatial studies of sulfur and background emission demonstrated that the optimum signal/background is obtained below the geometric center of the standard burner. The distribution suggested use of a monochromator with horizontal entrance slit rather than a filter. Unfortunately the distribution is not constant with time, being related to the buildup of deposits in the burner.

A study of the line emission of sulfur demonstrated that multiple slits could be constructed which would both increase specificity for sulfur and increase the usable signal. A comparison of the multiple slits with a single slit of the same spectral bandpass indicated an increase of about three in sensitivity.

The differential mode, using the multi-slits, was not so successful as hoped, for a variety of reasons. First, the quartz plate introduces some defocussing. Together with the slightly oversized slits employed, this resulted in decreased differential signal.

Defects in the burner and electronics of the standard instrument--beyond the province of this contract--limited the results to a demonstration of the successful implementation of the basic principles. Using multi-slits in the non-differential mode the final sensitivity was about an order of magnitude greater than the comparison standard instrument (or about three times more sensitivity for SO_2).

2. LABORATORY STUDIES

2.1 Standard Instrument Evaluation

The basic instrument supplied by EPA was a Melpar Model LL-1100-1B SO_2 Analyzer. As received the instrument was very difficult to ignite and demonstrated very poor sensitivity. The problem was traced to a leaking sample chamber, resulting in a reduction in the hydrogen/air ratio. While the problem was temporarily corrected by using a newer, higher quality O-ring and longer screws, it reoccurred during the entire project.

The close coupling of the pump and the sample/hydrogen sources resulted in very visible "bouncing" of the balls in the gas gauges. A simple expansion chamber, seven inches long and three inches in diameter, inserted between the pump and the instrument, increased flow stability and allowed better setting of flow valves. Subsequent work revealed that even then the flows could not be accurately reset using the gauges provided.

As the project progressed numerous leaks developed, particularly around the igniter and flame ionization detector feed-throughs. In each case the problem was fixed in a temporary manner; however, it is clear that the basic burner is not reliable.

2.2 S_2 Emission Studies

To modify the instrument for spatial studies of the combustion chamber, we were able to reorientate the combustion chamber, heated exhaust manifold and inlet tubing without shortening any pieces or changing heaters. With the instrument cover removed, the combustion chamber was positioned on the left side of the instrument, oriented so it could be viewed by a monochromator. It was then a simple matter to restore the instrument to its original condition for comparison.

The burner was mounted on a cross-slide allowing precise positioning (±0.1mm) in frong of a $1mm^2$ aperture; in turn, a quartz lens imaged the aperture on the entrance slit of a Farrand monochromator. The aperture

selected a small area of the flame region. Various removable stops near the lens allowed selection of angular field of view. This arrangement allowed versatile spatial scanning of the combustion region at intervals of lmm and was used for both S_2 and flame background monitoring.

Using the NBS SO_2 permeation tube provided, a concentration of approximately 1 ppm was used for most studies. First measurements consisted of horizontal and vertical spatial scans across the burner with the monochromator set at an S_2 emission peak. (At 1 ppm SO_2 flame background is no problem.) Figure 1 shows a typical set of raw data from a raster of vertical scans over the combustion chamber. The circle in the upper right hand corner represents the combustion chamber (dimensions X2). The square protruding from the bottom represents the flame shield; the nib on the left is the igniter; the line proceeding from the right hand wall represents the (unused) flame ionization detector. The vertical scans are identified at the top of the combustion chamber. In the graphs the x-dimension indicates the vertical distance from bottom to top (X2).

The data of Figure 1 indicate the variation of S_2 emission. Of particular interest are the dips in emission corresponding to the igniter and the flame ionization detector. Thus, Curve 2 (left-most group) shows the effect of the igniter while the effect of the larger FID element shows up in many traces. It is evident that the greatest S_2 emission occurs below the horizontal centerline and very close to the flame shield.

Using data such as in Figure 1 and corresponding horizontal scans, we had hoped to plot contour graphs of equal emission; however, it was found that by the time we completed a set of scans we could no longer reproduce the first scan in amplitude. Thus, the data were unsatisfactory. The non-repeatability could have been due in part to the short-term stability of our SO_2 source, but was mostly due to actual changes within the burner.

The contour graphs of Figure 2 were obtained by selecting a particular emission level and scanning both x and y directions to find all positions for

the given level. In this way the time to complete a given contour was short, and it was found the contours did form closed loops. Longer term changes would be reflected in relative error between contour levels.

Contour graphs such as these showed quite unequivocally that there is a large variation in S_2 emission over the burner; and if Figure 2 were representative, it would suggest using a horizontal slit across the two peaks, or an off-center aperture for use with a filter.

Unfortunately it was found that the pattern of flame emission varies, within hours, over a wide range, due to turbulence in the flame and build-up of a deposit on the inner walls of the combustion chamber. After the chamber has been disassembled and cleaned, the emission pattern again shows a big change. In Figure 3 we show contours obtained at a slightly later date which show a large asymmetry in emission. In general, it was found that the emission pattern depended strongly on the build-up of materials within the burner.

Other studies included the effect of angular field of view on the emission pattern and on the changes associated with removal of the FID element (which is not used). While it is clear that protrusions such as the FID element or the igniter do affect the patterns, the variability with buildup of deposits made it impossible to form a clear picture of the effect of the protrusions.

In Figure 4 we indicate typical S_2 emission as a function of wavelength using 2 nm spectral resolution on the monochromator, a 2mm slit aperture at the face of the burner and approximately 2 ppm SO_2. In Figure 5 we illustrate the relative signal and background using 5 nm spectral resolution and an SO_2 concentration of approximately 0.5 ppm. In Figure 6, the spectral resolution is also 5 nm but concentrations vary from approximately 1 to 0.3 ppm.

The signal appearing at approximately 310 nm in both Figures 5 and 6 is the most prominent flame background, probably due to (OH). Comparing

the center trace of Figure 6 and Figure 5 (identical spectral resolution and SO_2 concentrations), it is evident that the flame peak at 310 nm is much more pronounced relative to S_2 in Figure 5 than in Figure 6. Figure 5 was taken at the geometrical center of the burner and flame--the region emphasized by the standard Melpar unit. Figure 6 was taken in a region exhibiting best S_2 emission. It is quite clear that the signal/background is far from optimum at the center of the burner.

2.3 Background Emission Studies

Figures 5 and 6 revealed the principal background signal at 310 nm. In Figure 7 we show a typical background trace showing the 310 nm signal and further emissions peaked at about 350 nm and very broadly at about 400 nm. In this case the spectral bandwidth has been increased to just over 10 nm, in order to increase sensitivity. From Figures 6 and 7 we find that the ratio of the highest S_2 peak to the corresponding background is about 800:1 for the 0.5 ppm SO_2 concentration. Since the S_2 signal depends on the square of the SO_2 concentration, the background is equivalent to approximately 0.02 ppm SO_2. While this is only an estimate, it establishes some idea of background limitations. This background does not change much when our laboratory air is filtered through charcoal.

The data of Figure 7 were obtained using a cooled 1P28 photomultiplier tube. Using an uncooled tube the electronic background interfered with flame background determination. Thus, for optimum sensitivity the photomultiplier may have to be cooled, although this requirement may be mitigated by eventual optimization of the optical system. In the standard Melpar unit the cathode of the photomultiplier is actually heated because of close proximity to the burner chamber! This may well account for the instability and drift observed during normal operation.

Figure 8 depicts the spatial distribution of the 310 nm background emission, using a measurement setup similar to that used for the S_2 contours, but with spectral bandwidth just greater than 10 nm. Contrasting this

set of contours with the S_2 emission contours of Figure 2, it is obvious that it should be possible to select regions with optimum signal/background ratios. In Figure 2 the maximum S_2 emission occurs at two points, both about 4mm below the geometric center of the burner chamber, near the corners of the flame shield. The flame background peak, on the other hand, is located above the centerline of the burner.

The original instrument has a 5.5mm diameter aperture in front of the burner. This is indicated on both Figure 2 and Figure 8. It is apparent that it does not include the major sulfur peaks, but is closer to a background peak. Since the system accepts a divergent beam (about 12°) broader areas of the flame are actually viewed.

Unfortunately a final signal/background plot (i.e., data of Figure 2 divided by data of Figure 8) cannot be made because the distributions change within the burner.

The chief background of interest is actually not the 310 nm emission (which occurs on the short wavelength side of the S_2 emission) but the 350 nm peak and the broad peak to longer wavelengths. The 310 nm peak was used for our measurements because of its greater intensity; however, an independent measurement indicated that the 350 nm peak occurs in the same spatial position as the 310 nm peak.

2.4 Choice of Monochromator System

As a result of the signal/background studies it was determined that the chief emission regions for S_2 occurred near the edges of the flame shield, somewhat below the centerline of the flame chamber; whereas the background peaked above the centerline of the burner. The optimum viewing region would then be below the centerline and include both S_2 maximum emission regions. This could be accomplished using a monochromator with its entrance slit horizontal and in the plane of the emission maxima. Or it could be accomplished by viewing only one maximum by means of a lens and an interference filter. Both systems would allow background subtract;

however, the filter system would be restricted to one line of S_2 emission with resulting loss of sensitivity and specificity. The monochromator was to be preferred for the above reasons plus the versatility of tuning which might allow application of the same instrument for other materials, e.g., phosphorus.

With the project officer's concurrence it was decided to incorporate the Farrand monochromator, used in the studies of sections 2.3 and 2.4, into the final instrument.

2.5 Multiple Slit Studies

The Farrand single monochromator has a tuning range from 200-700 nm and a dispersion of 11 nm/mm. With exit slit removed the exit aperture is approximately 6 mm, corresponding to a spectral width of approximately 66 nm. From Figure 4 it is evident that the six major S_2 peaks could be imaged simultaneously if the monochromator is set at 378 nm. The average distance between the major peaks is 10 nm; however, line shapes are not identical and it is desirable to tailor a mask to fit the actual emission lines as observed by a monochromator.

The entrance slit will determine the spectral resolution of the monochromator. In order to determine the optimum setting, pictures were taken of the S_2 emission lines at the exit plane of the monochromator. Entrance slits of 2 nm, 3.5 nm (fabricated specially) and 5 nm were employed for the data of Figure 9, the monochromator being set at 380 nm for the 2 nm slit and at 378 nm for the wider slits. SO_2 concentrations were approximately 1 ppm for the 2 nm slit and 0.75 ppm for the others. From data such as these it was decided to employ a 3.5 nm entrance slit to compromise between higher sensitivity and adequate separation to allow measurements between the peaks for background subtract. Using separations measured from the photographs, 3.5 nm slits were etched in brass for use in the exit position of the monochromator.

2.6 Background Subtract Mechanism

In one mode of operation the S_2 peaks and valleys are to be imaged alternately on the multi-slits in order to subtract background and increase specificity. Several possible methods were investigated including oscillation of the multi-slits in the monochromator focal plane, rocking the grating to move the emission image across the multi-slits, and rotation of a quartz plate in the monochromator to move the image. The last method was selected for simplicity of mechanical operation and least interference with monochromator tuning.

A 2 mm quartz plate was mounted in the exit beam of the monochromator, just before the multi-slit. The monochromator was tuned so that the six strongest S_2 lines registered on the multi-slits when the quartz plate was oriented perpendicular to the beam. As the plate is rotated in the beam the S_2 lines are displaced until they are not transmitted by the multi-slits. The quartz plate was driven by a 10 watt 115 volt a.c. synchronous motor, through a gear train, to oscillate at from 15-18 oscillations per minute. Oscillation is caused by an eccentric groove in the gear face which has a pin connected to a guided slide. A pin in the slide connects to a bell crank on the quartz plate holder. The bell crank has a slot for the connecting pin to allow for angular adjustment of the quartz plate.

2.7 Electronic Modifications

While it was desired to use as much of the original electronics as possible, it was not feasible to use the original package. The original amplifier had too long a time constant as compared to the chopping period. A new electronic package was developed which has a wide-band pre-amplifier stage, a synchronous demodulator, an output filter with time constants of 0.1, 1.0 and 10 seconds, and two stages of additional amplification. The full scale sensitivity is from 10^{-4} to 10^{-10} amps. Provision was made for the addition of a log linear amplifier at a later date.

The first stage of the three-stage amplifier consists of an Analog Devices 310J operational amplifier with associated feedback resistor to make a transresistance circuit. The output of this stage passes through a mechanical chopper synchronized with the optical chopper so that the desired S_2 signal is detected when the quartz plate is perpendicular to the optical beam. The chopped output is applied to the positive and negative inputs of an AD43J Analog Device through a time constant network. The AD43J is used as a differential detector with unity gain. The differential output is coupled to a Fairchild 741C amplifier which allows adjusting gain by a factor of six for calibration purposes. The output of the 741C is connected to a voltage divider, giving both one volt and one millivolt outputs. These outputs may be used to drive appropriate high impedance recorders or a voltmeter. Schematics are given in Fig. 10.

During the course of our measurements we often used laboratory high voltage and low voltage supplies in preference to the supply incorporated in the Melpar unit. The built-in high voltage supply had a 120 cycle ripple which contributed to background. However, for final test we returned to the built-in supplies, since they sufficed to demonstrate the operation of the modified instrument.

2.8 Laboratory Measurements

During laboratory measurements prior to final assembly, after final assembly and at a demonstration at Research Triangle Park, many difficulties occurred with the basic instrument. These served not only to delay performance checks, but to make detailed signal/noise and sensitivity measurements difficult. The principal problems included recurring leaks about gaskets, igniter feedthrough and FID feedthrough, shorting out of block and exhaust heater control (necessitating a manual system), and somewhat unstable power supplies. As a result the laboratory measurements were often made with substitute amplifiers, etc. Nevertheless, they demonstrated the successful operational mode of the instrument.

2.8.1 Modes of Operation

The improved instrument will have several possible modes of operation. First the instrument may be used in a mode similar to the original instrument, using fixed single slits. These slits may be set to match a particular line, or may be wide enough to encompass some or all of the lines. For extreme sensitivity (and least specificity) the bandpass may be greater than 60 nm and include all six major lines.

The instrument may also be used with the multi-slits in the output to give better specificity for S_2 emission. The entrance slit may be matched to the multi-slit (3.5 nm) for best specificity, or increased to 5 nm for increased sensitivity. This mode is still non-differential. The quartz plate is adjusted perpendicular to the beam and the oscillator is not used.

Finally, using the multi-slits and a suitable entrance slit, the oscillator may be used, and the output is the smoothed difference between measurements at S_2 peaks and valleys. This last should offer the highest specificity against interferents, with some loss of sensitivity.

The above discussion describes the application of the instrument to sulfur detection. By tuning the monochromator to other wavelengths, and with suitable selection of slits, the instrument is applicable to other materials, e.g. phosphorus.

2.8.2 Single Slit Mode

It is usually best to match input and output slits of the monochromator. In Fig. 4 we displayed the spectral scan of a 2 ppm concentration of SO_2 viewed with 2 nm slits. It will be observed that the lines are well resolved, with minima not far from the base. Fig. 11 contains similar data for 3.5 nm slits and a concentration of 0.5 ppm. The sensitivity is clearly higher while the resolution remains fairly good. The minima approach the base less closely than in Fig. 4. Finally, Fig. 12 shows similar data for 5 nm slits. The overall signal is greater, but there is now a large unresolved envelope.

For greatest sensitivity (at the loss of specificity) even larger slits could be used. Thus using 20 nm slits produces about four times greater signal than 10 nm slits.

2.8.3 Multi-Slit Mode

Using the line separation data of Fig. 9 and 3.5 nm spectral width, multi-slits were constructed for the six largest central lines of S_2 emission. (Grooves were first milled into an aluminum block and photographed. Slits were then etched in a nickel-plated copper of 0.003 inch thickness.)

The results were checked by comparing the throughput using the 3.5 nm entrance slit and multi-slits (with the monochromator set to pass the six lines), and the throughput using 3.5 nm single entrance and exit slits. These results are indicated in Fig. 13. Here the lower trace shows single-slit output while the upper curve shows a scan through the maximum for the multi-slit mode. Gain is the same for both traces. The increase in sensitivity for monitoring six lines over the single largest line (measured by peak height) is about three, which is somewhat lower than if all lines were imaged perfectly. The increase is also about three if a peak to valley measurement is used. We note that the minima using multi-slits are not quite so deep as hoped for, indicating the multi-slits are not perfectly designed. As will be discussed later, there is also a loss of image definition caused by the quartz plate.

We have also obtained data for various larger entrance slits used in conjunction with the multi-slits. The output increases more or less linearly with input slit aperture; however, specificity is lost rapidly (as measured by minima when tuning with multi-slits in place).

2.8.4 Multi-Slit Differential Mode

In this mode the signal is sampled alternately when the S_2 peaks are imaged onto the multi-slits, and when they are shifted approximately 5 nm. The sampling period is approximately 30° for both peaks and valleys, phasing being accomplished by mechanical positioning of a reed switch. From the

data accumulated it appeared best to use a 5 nm fixed entrance slit in combination with the 3.5 nm multi-slits. (Spectral widths can be translated into actual dimensions using the dispersion of 11 nm/mm.)

Using filtered sample air, the output is set to zero by adjusting the reed switch. S_2 emission is then read as before. Filtering is accomplished after difference measurements. Signal to noise is decreased not only because of the use of narrow slits but because of the short duty cycle. (Information is gathered for approximately one-sixth of a cycle.)

Fig. 14 is a tracing of cycling through a 10 ppb SO_2 sample and filtered laboratory air. The sensitivity of the instrument is set at 10^{-8} amperes full scale and a 10 second time constant is used. The low-frequency noise is attributable largely to the variation in phasing in the device, although power supply instability is also evident.

2.9 Instrument Packaging and Controls

With some rearrangement of components it was possible to utilize the original instrument case. Side access holes had to be added to incorporate the quartz plate drive mechanism and allow slits to be changed. The original front panel was used, with relabeling of switches to conform to new functions. The final instrument is pictured in Figures 15-17.

In Fig. 15 we see the instrument with right panel removed, showing the new electronics sub-chassis as well as the original front panel. Figure 16 shows a view of the left panel with quartz-plate oscillating mechanism and slit access holes. A metal dust cover for the drive assembly has been removed. Finally, Fig. 17 is a top view showing the layout of principal components. The necessary rearrangements of components will be discussed below.

2.9.1 Electronics

The new electronic package has the same overall dimensions as the original. The amplifier is mounted in a shielded subassembly, with three access holes to adjust amplifier offset and gain. The subassembly is mounted directly to the rear of the front panel, utilizing the original cut-outs. The original scales apply to the internal calibration and to all amplifier settings except the log linear (which is omitted). The original two-position time constant toggle switch has been replaced with a four-position switch. The first three positions allow time constant selection of 0.1 seconds, 1.0 seconds and 10 seconds. The fourth position allows conversion of the instrument from the differential mode to a straight-through amplifier. See Fig. 15 for details.

2.9.2 Burner, Monochromator and Photomultiplier Detector

The bulk of the monochromator necessitated repositioning of several components. The monochromator is mounted so that the entrance slit is horizontal and looking at the lower center region of the burner. The burner is mounted directly onto the monochromator with an asbestos gasket for thermal isolation. The exit slit of the monochromator faces upwards, necessitating the addition of a front-surface aluminized mirror to couple the output to the original photomultiplier tube. The latter is now mounted horizontally to fit into the original enclosure. This part of the layout can be seen in Fig. 17. Both entrance and exit slits can be replaced through openings in the left side of the cabinet (Fig. 16). Standard slits of 2, 5, 10 and 20 nm together with a special 3.5 nm slit can be used in the entrance position. The exit position can utilize either the special multi-slit or any of the above.

The monochromator dial indicator has been modified with a fine tuning adjust located in the center of the calibrated dial to allow changes as small as 0.1 nm. With the fine adjust in its maximum counterclockwise position the center wavelength is as indicated on the large dial. The fine tuning adjust knob can be seen in Fig. 17: it is available only with the top to left side cover removed.

The burner position was changed from rear center to front left center to allow mounting on the monochromator. Exhaust lines had to be changed to accommodate the new burner location; however, the location of the sample control valve did not change, and the same rear panel location was used for the connection of the exhaust to the pump.

The temperature control was relocated to allow space for the monochromator and to make adjustment of the temperature convenient.

The sample air and hydrogen inputs were moved from the rear panel to the front left side, reducing the length of the connecting hose to the flow indicators to approximately 8 inches. This reduction reduces recovery time with large sample concentration changes and minimizes contamination of lines.

2.9.3 Quartz Plate Drive Mechanism

It was necessary to mount the motor and gears for the oscillating quartz plate mechanism outside of the original case. This can be seen in Figs. 16 and 17. The unit is normally covered with a metal dust shield. The oscillating mechanism can be deactivated by means of a toggle switch on the rear panel, allowing use of the instrument in the original non-differential mode.

2.10 Delivery Demonstration at Research Triangle Park

The demonstration at RTP was not so successful as we had hoped due to the recurrence of perennial problems with the basic instrument. A short time prior to the demonstration another leak developed in the igniter feedthrough. Previous trouble with the automatic block/exhaust heater forced use of a manual control. Upon arrival at RTP we found alignment of the quartz plate, etc., had been affected by shipment. Further, unknown to us at the time, a further leak had developed approximately equal in flow to sample intake.

The basic unit provided by RTP for comparison was an older model which proved far more stable than the unit originally supplied to us. Initial

measurements revealed our unit was far down in sensitivity ar. ' signal to noise. After intensive troubleshooting the instrument was demonstrated in its several modes as discussed earlier. The results of the test may be summarized as follows:

1. The incorporation of a monochromator in the FPD was successful in concept and execution. The versatility in choice of bandpass, single or multi-slits, and tunability, was demonstrated.

2. The limitations of the performance of the revised instrument can be traced to recurrent leak problems in the sampling system and a poor burner geometry for coupling to the monochromator.

3. After troubleshooting on the spot, the final sensitivity and signal/noise ratio of the revised instrument were slightly superior to those of the comparison instrument. Multi-slits in the non-differential mode were used for this comparison.

4. The differential mode had considerably less sensitivity than the non-differential.

5. Selectivity comparisons were inconclusive due to long sampling lines and uncontrolled sampling me thods.

Subsequent to the demonstration the large unknown leak was found and repaired, increasing sensitivity and signal to noise by about an order of magnitude.

3. DISCUSSION AND RECOMMENDATIONS

The principal objective of this contract was to increase the optical efficiency of the Melpar flame photometric detector for the detection of SO_2. Such increased efficiency should lead to higher sensitivity, stability and freedom from interference. Two routes were explored. First, the spatial distribution of sulfur and background emission were plotted to determine regions of greatest signal/background. Second, multi-slits were constructed to match the structured sulfur emission and allow background subtract.

An assumption made at the beginning of this work was that the basic instrument, including electronics and burner, was well designed and that we would not attempt to improve on it. Our experience has proven this false, since we have had to patch up innumerable leaks and make do with an inadequate burner.

The spatial studies of sulfur and background emission demonstrated that the optimum signal/background is obtained below the geometric center of the standard burner. The distribution suggested use of a monochromator with horizontal slit rather than a filter. Unfortunately the distribution is not constant with time, being related to the buildup of deposits in the burner.

While the signal/background ratio is increased with the monochromator, the total light input is decreased considerably, limiting any dramatic increase in sensitivity. The obvious next step is to redesign the burner to maximize coupling of signal to a monochromator slit.

A study of the line emission of sulfur demonstrated that multiple slits could be constructed which would both increase specificity for sulfur and increase the usable signal. A comparison of the multiple slits with a single slit of same spectral width indicated an increase of about three in sensitivity. The multi-slits fabricated at Baird-Atomic are not optimum; however, they demonstrated the correctness of the principle.

The differential mode, using the multi-slits, was not so successful as hoped, for a variety of reasons. First, the method chosen to shift the spectrum across the multi-slits involved some difficulty. The quartz plate introduces some defocussing. Further, phasing, or balancing of peak and valley signals, was not well enough controlled using reed switches, resulting in some instability. Finally, the greater bandwidth required resulted in increased noise. A further consideration involves choice of slit widths. For the non-differential application of multi-slits a 5 nm entrance slit and 3.5 nm multi-slits were chosen as a good compromise between high specificity and high throughput. In the differential mode it would have been better to use narrower slits since peak-valley differences are quite sensitive to spectral width and precision of registration.

A plague of burner leaks and electronic problems in the basic instrument, particularly in the latter part of the study, made it impossible to determine the increase in sensitivity afforded by the innovations introduced. Using a 5 nm entrance slit and a 3.5 nm multi-slits in the non-differential mode, the demonstration showed a better signal/noise than the comparison standard instrument. The test data were not precise, but suggest an improvement of about a factor of three. Since this measurement was made with an unknown leak present, we feel the improvement was probably well over an order of magnitude.

In conclusion, the work of this contract has successfully demonstrated the use of a monochromator and multi-slits to increase both the optical efficiency and specificity for sulfur detection in a standard flame photometric detector.

3.1 Recommendations

Based on the results of this program the following recommendations are made to realize fully the potential of techniques developed:

1. Redesign the burner to optimize coupling between sulfur emission and a monochromator slit.

2. Redesign the burner to improve flame stability and eliminate leaks.

3. Evaluate improvement in signal/noise and establish minimum detectable level of SO_2.

4. Investigate applicability of instrument to other materials, e.g., phosphorus, arsenic and selenium.

4. OPERATIONAL PROCEDURES

Because of the similarity to the basic Melpar unit, most operational procedures are similar to those for the model LL-1100-1B SO_2 Analyzer. Reference should be made to the Instruction Manual, especially Section III.

4.1 Operating Controls

a. H_2 Flow Control	Same
b. Sample Air Flow Control	Same
c. Power Switch	Same
d. Ignition Switch	Same
e. Temperature Control	Same, but relocated
f. Range Selector	Same, but no LOG position
g. Calibrate Switch	Same
h. Time Constant	Changed to rotary switch with time constants of 0.5 sec, 1 sec and 10 sec. Two spare positions available for other time constants.
i. Buckout	Same
j. Thermocouples	Same (but temperature control is manual using a Variac)

4.2 Operation Start-Up

a. Set-up Provisions	Same, except set RANGE SELECTOR switch to appropriate linear scale.
b. Operation	All items the same except linear scale only.

4.3 Recorder Input

Same, except omit reference to LOG position.

4.4 Calibration

Final calibration incomplete due to various possible modes of operation and difficulties with basic instrument.

4.5 Gas Flow System — Same (Section IV of Melpar manual)

4.6 Maintenance — Same (Section V of Melpar manual)

4.7 Differential Mode

The differential mode is in operation when the chopper toggle switch on the rear of the instrument is in the on position.

To shift from differential mode to straight operational mode, turn chopper switch off. Remove dust cover on chopper assembly and rotate chopper drive so that the upper reed switch is in a closed position. The detector output is then connected directly to the operation amplifier for a direct output to recorder. The chopper switch in off position closes operational amplifier positive input to ground.

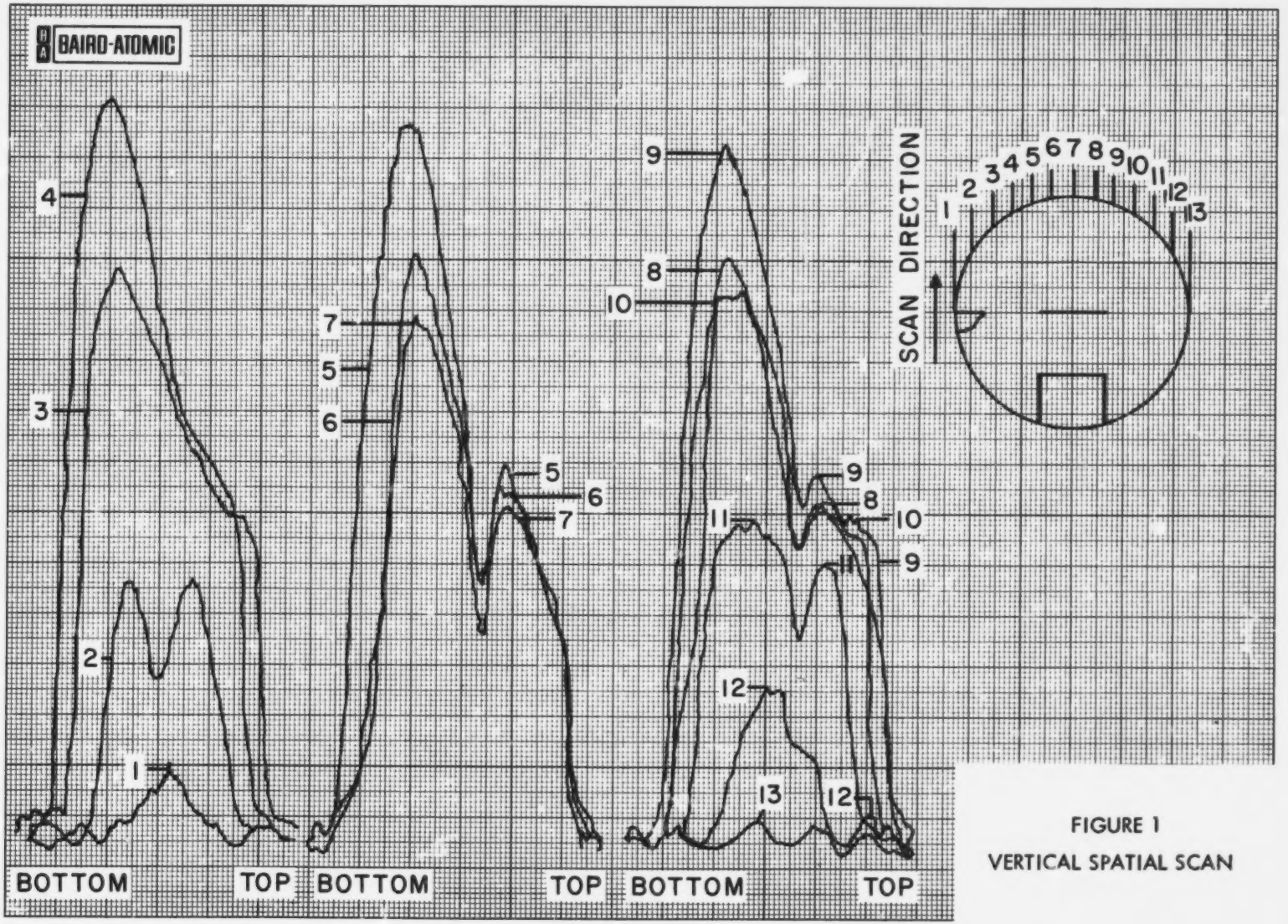

FIGURE 1
VERTICAL SPATIAL SCAN

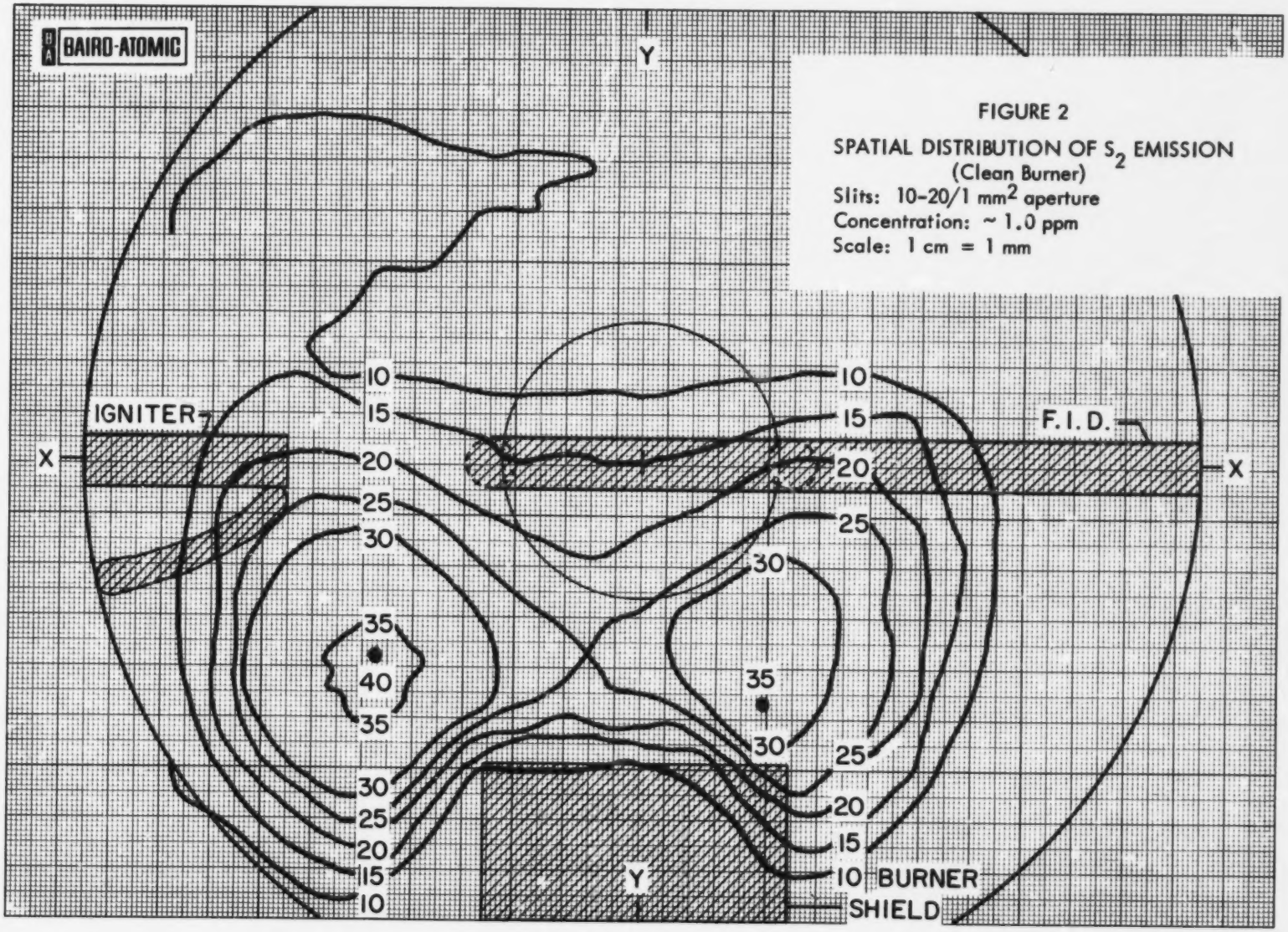

FIGURE 2

SPATIAL DISTRIBUTION OF S_2 EMISSION
(Clean Burner)
Slits: 10-20/1 mm^2 aperture
Concentration: ~ 1.0 ppm
Scale: 1 cm = 1 mm

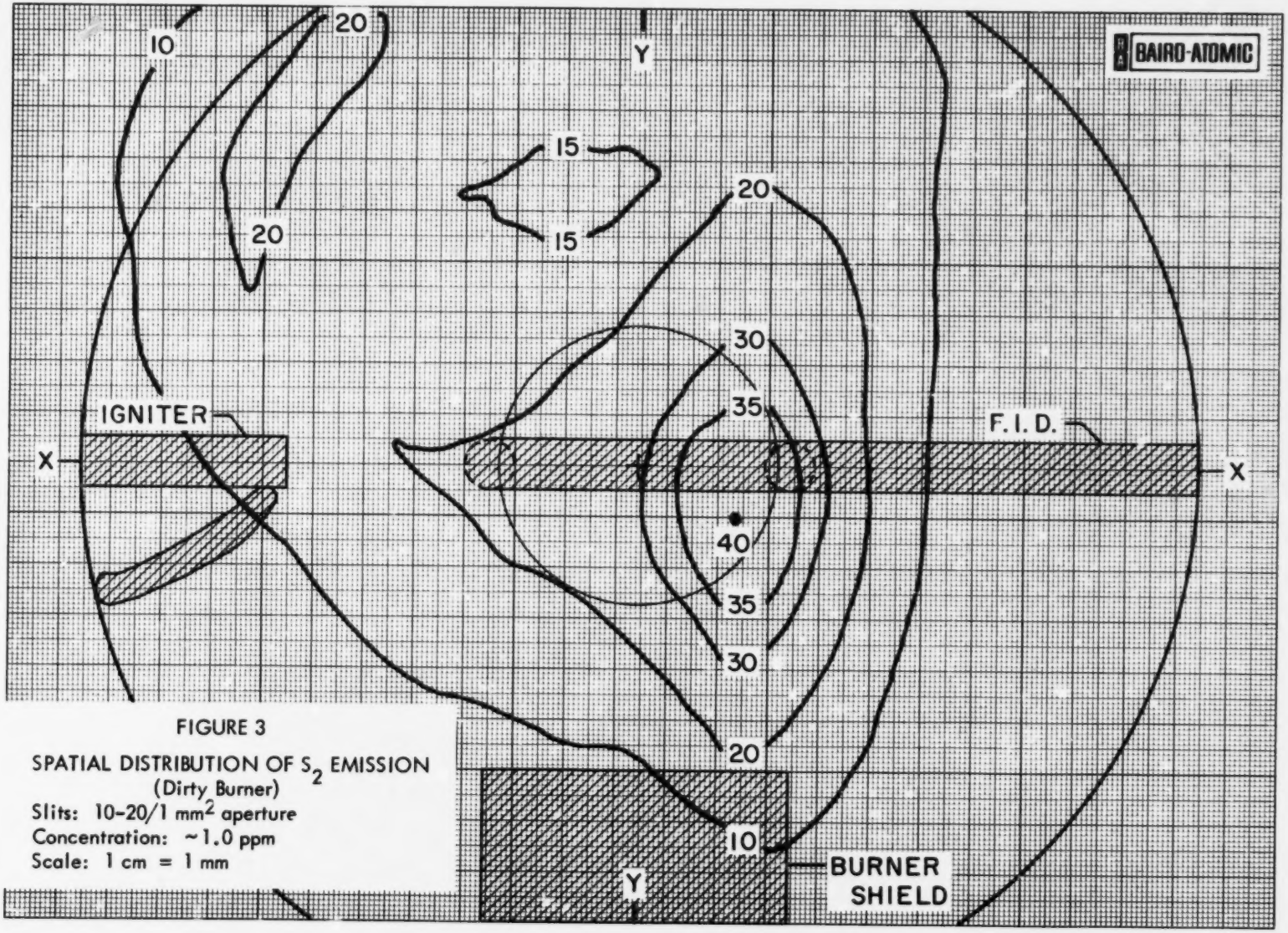

FIGURE 3

SPATIAL DISTRIBUTION OF S_2 EMISSION
(Dirty Burner)
Slits: 10-20/1 mm^2 aperture
Concentration: ~1.0 ppm
Scale: 1 cm = 1 mm

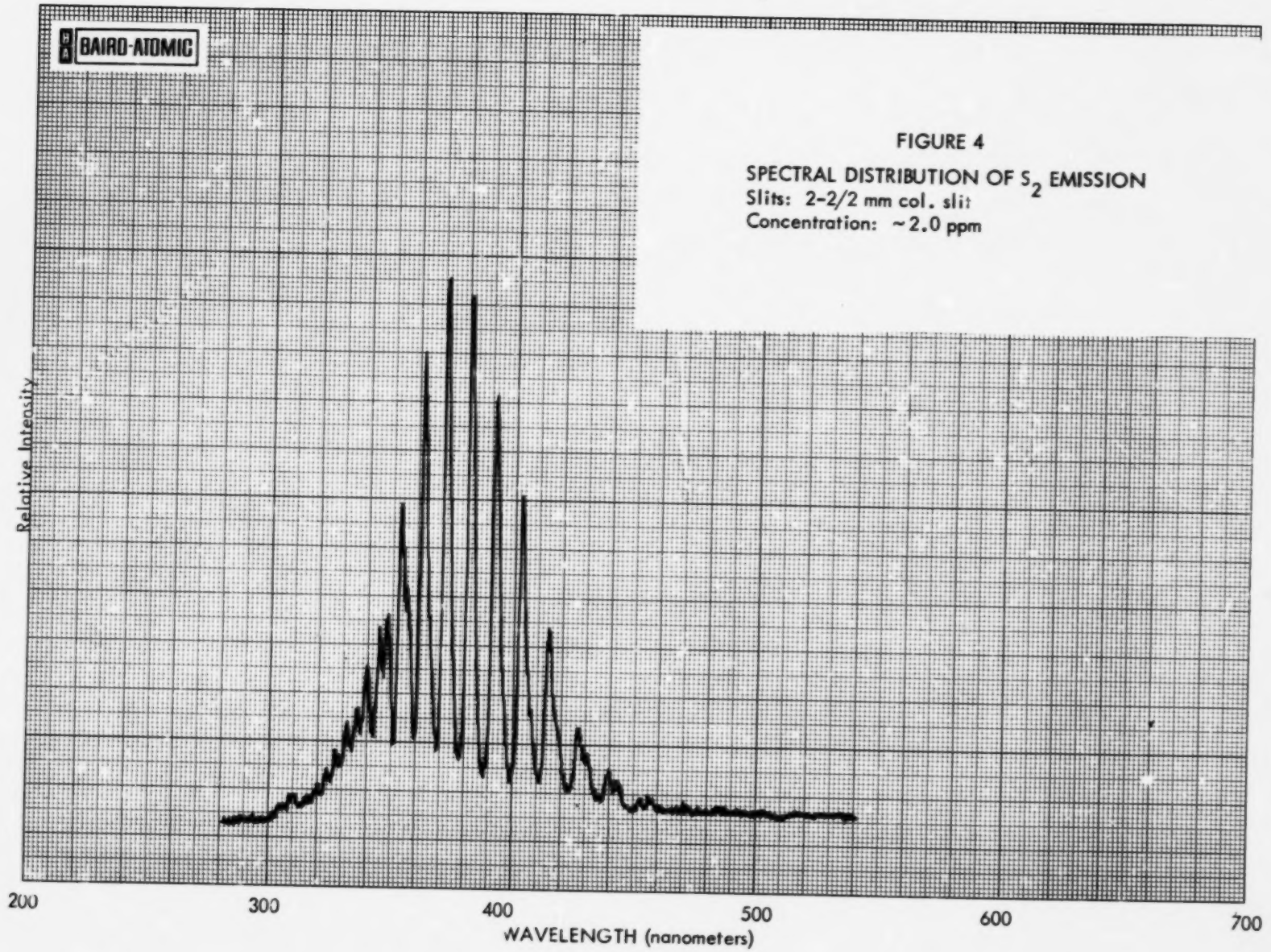

FIGURE 4

SPECTRAL DISTRIBUTION OF S_2 EMISSION
Slits: 2-2/2 mm col. slit
Concentration: ~2.0 ppm

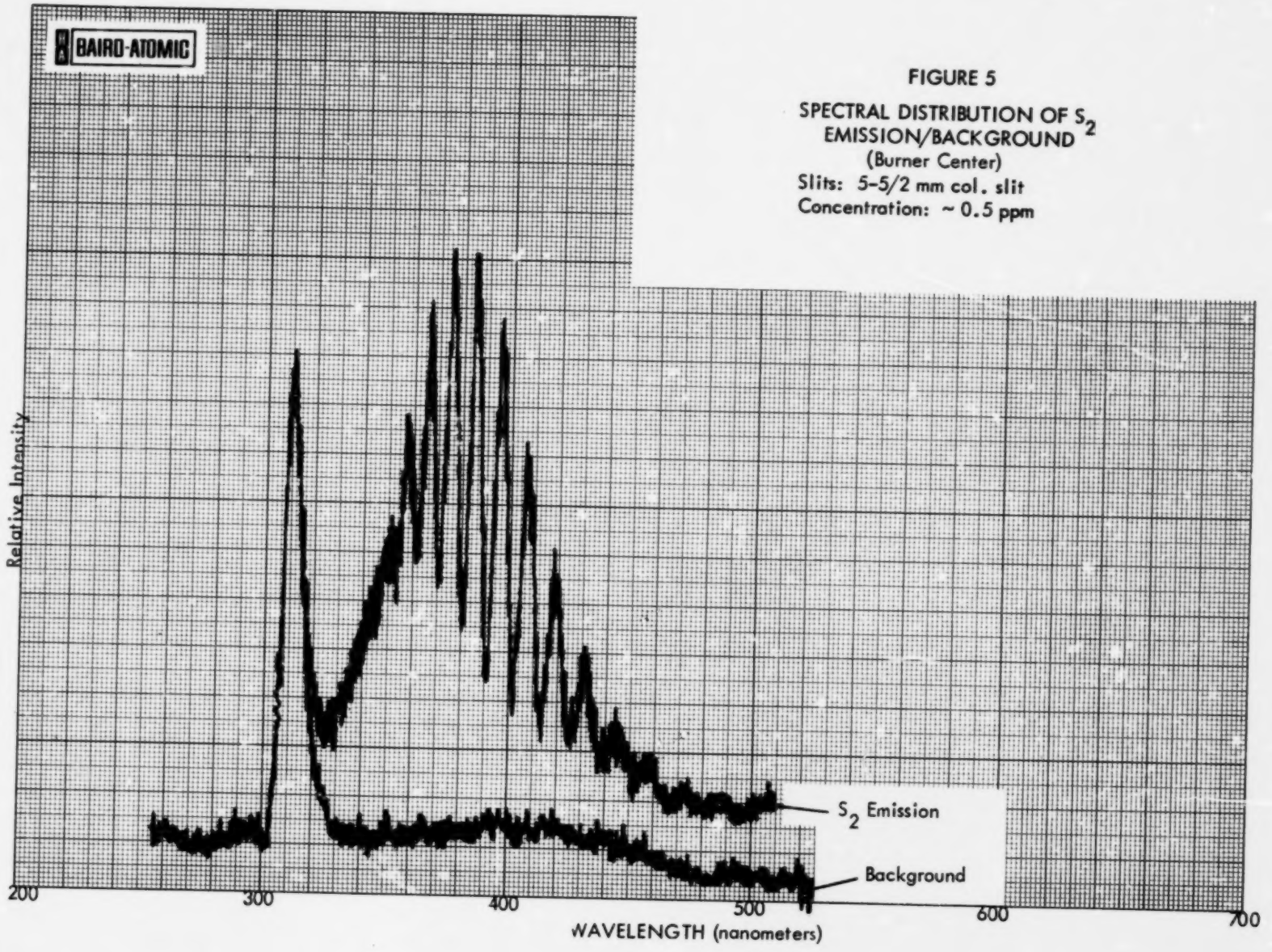

FIGURE 5

SPECTRAL DISTRIBUTION OF S_2 EMISSION/BACKGROUND

(Burner Center)

Slits: 5-5/2 mm col. slit

Concentration: ~ 0.5 ppm

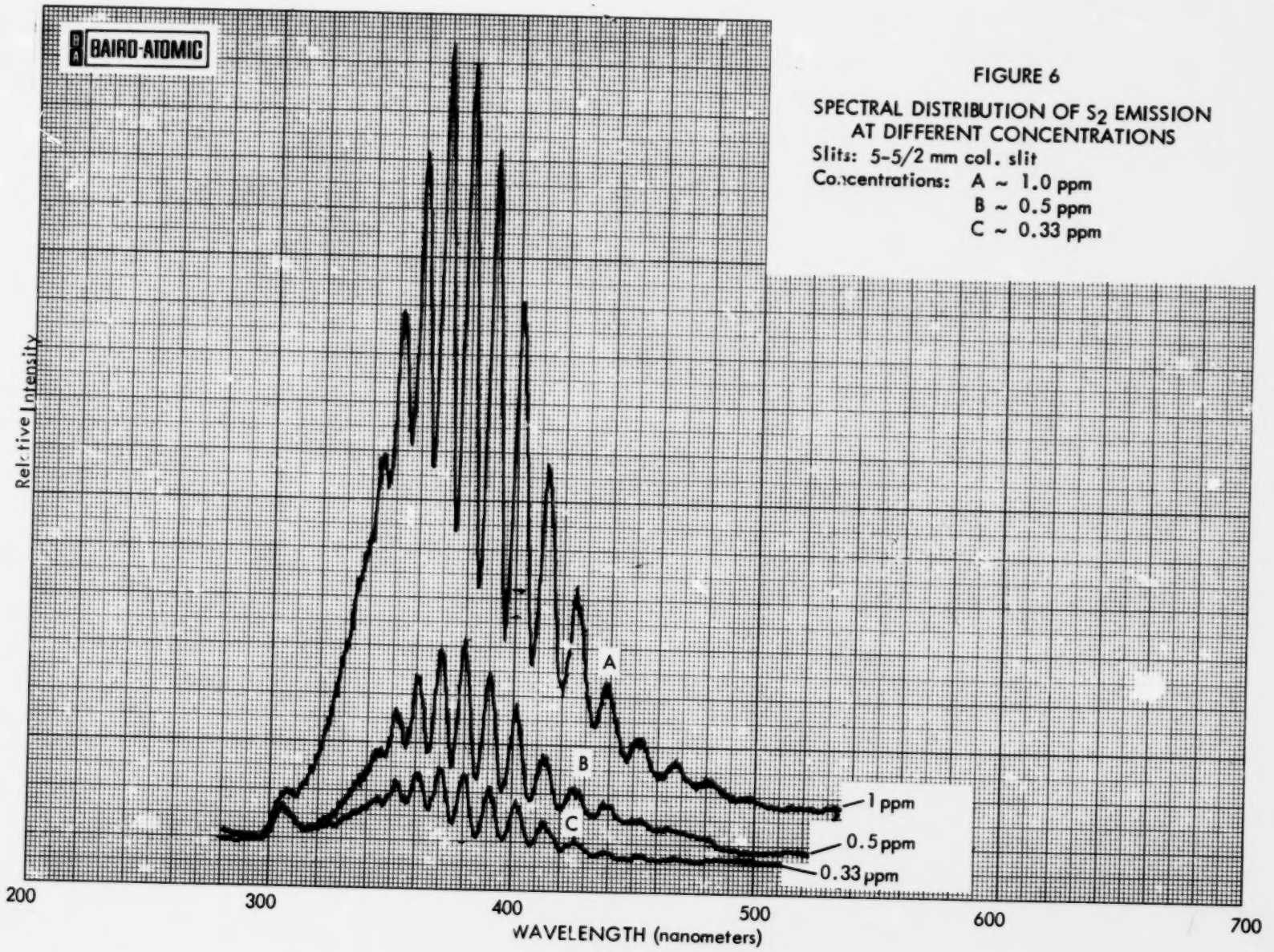

FIGURE 6

SPECTRAL DISTRIBUTION OF S_2 EMISSION AT DIFFERENT CONCENTRATIONS

Slits: 5-5/2 mm col. slit

Concentrations: A ~ 1.0 ppm
B ~ 0.5 ppm
C ~ 0.33 ppm

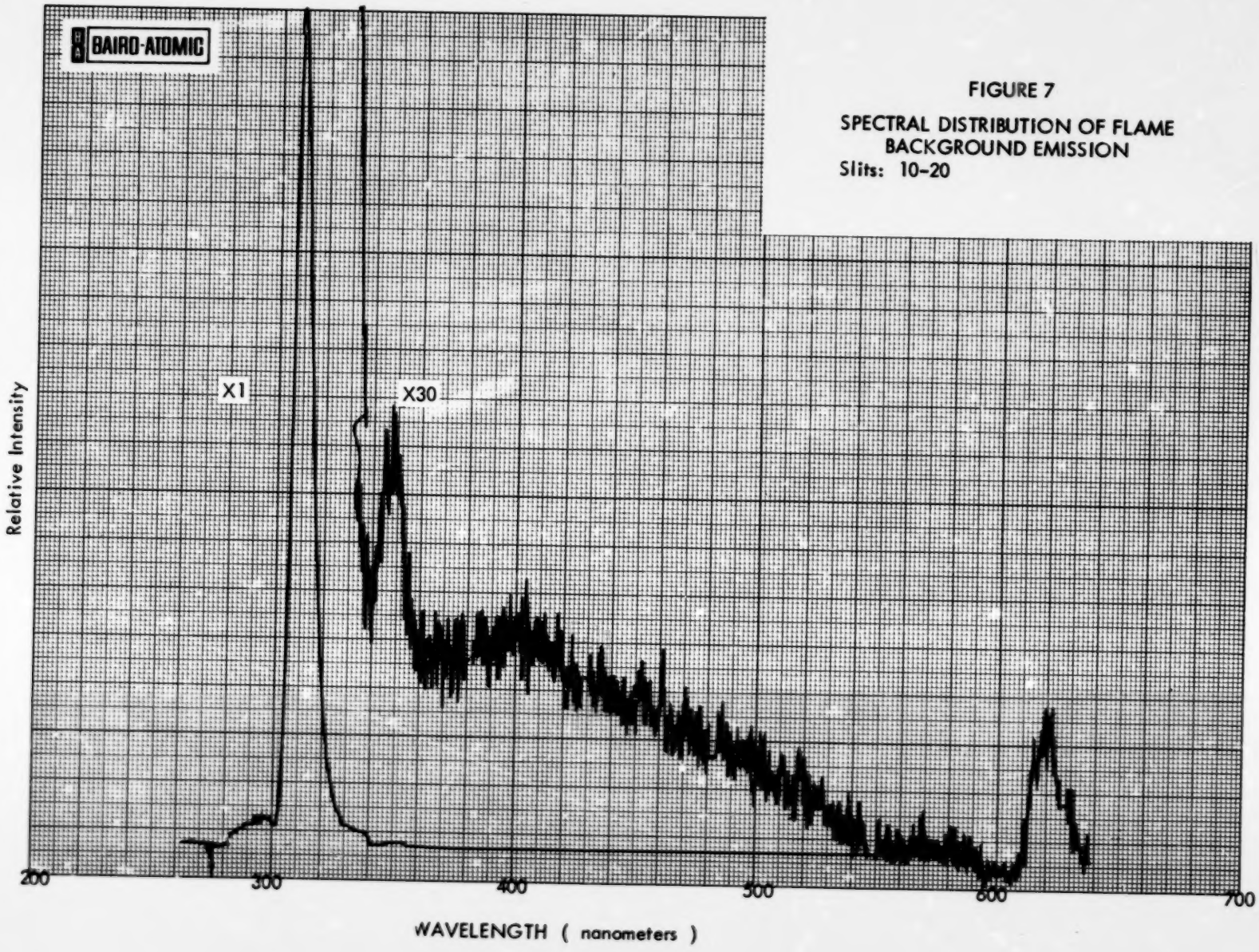

FIGURE 7

SPECTRAL DISTRIBUTION OF FLAME BACKGROUND EMISSION

Slits: 10-20

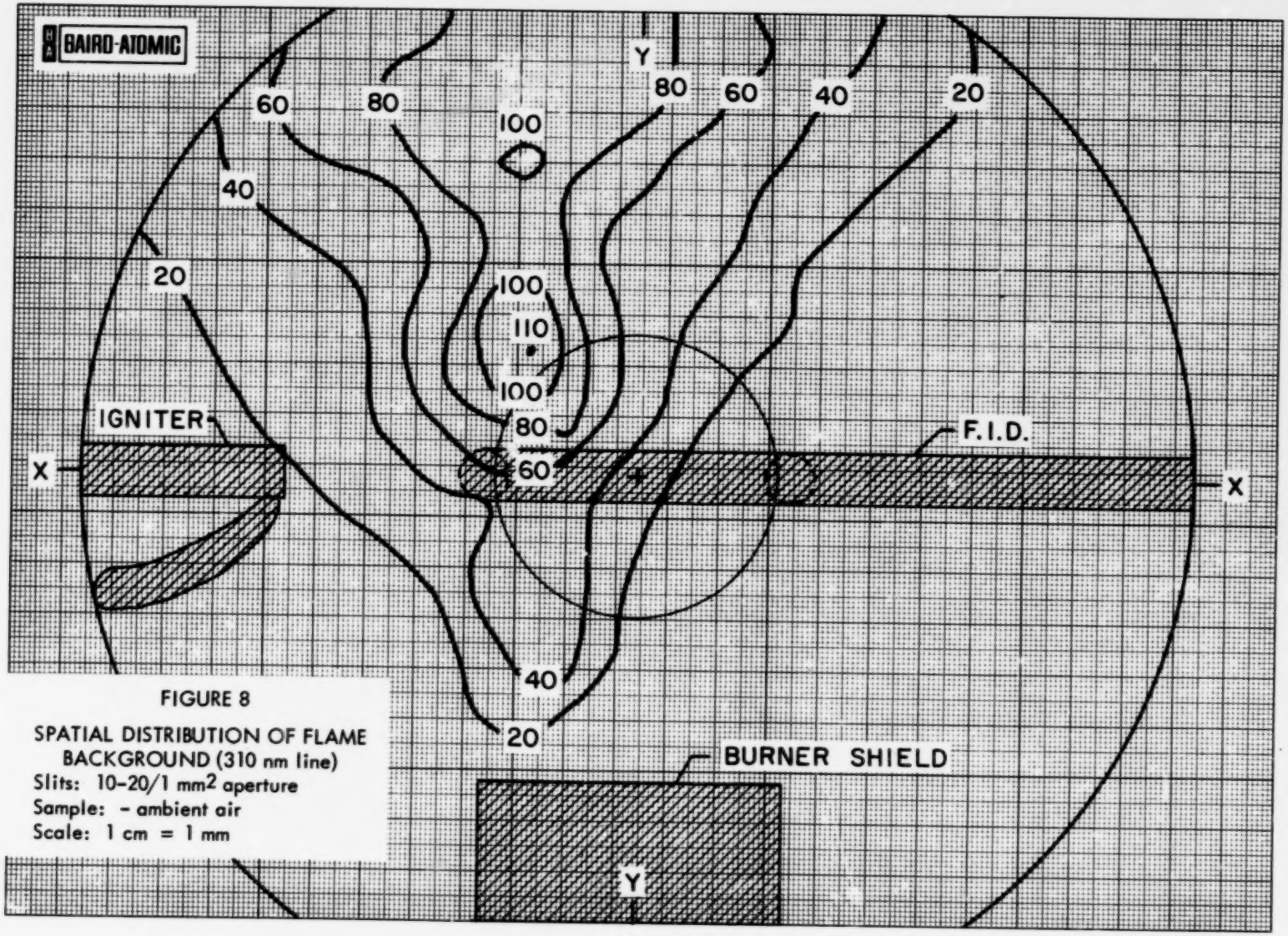

FIGURE 8

SPATIAL DISTRIBUTION OF FLAME BACKGROUND (310 nm line)
Slits: 10-20/1 mm^2 aperture
Sample: - ambient air
Scale: 1 cm = 1 mm

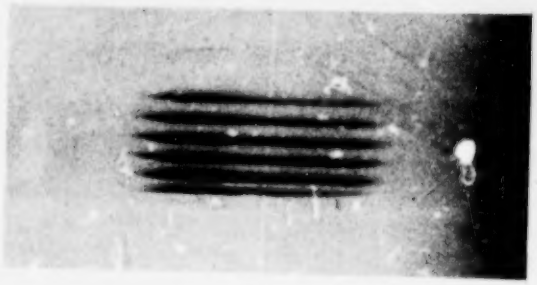

2 nm entrance slit,
1.0 ppm SO_2, 380 nm center wavelength

3.5 nm entrance slit,
0.75 ppm SO_2, 378 nm center wavelength

5 nm entrance slit,
0.75 ppm SO_2, 378 nm center wavelength

photos enlarged 3X

Figure 9. S_2 spectra at exit plane of monochromator for different entrance slits

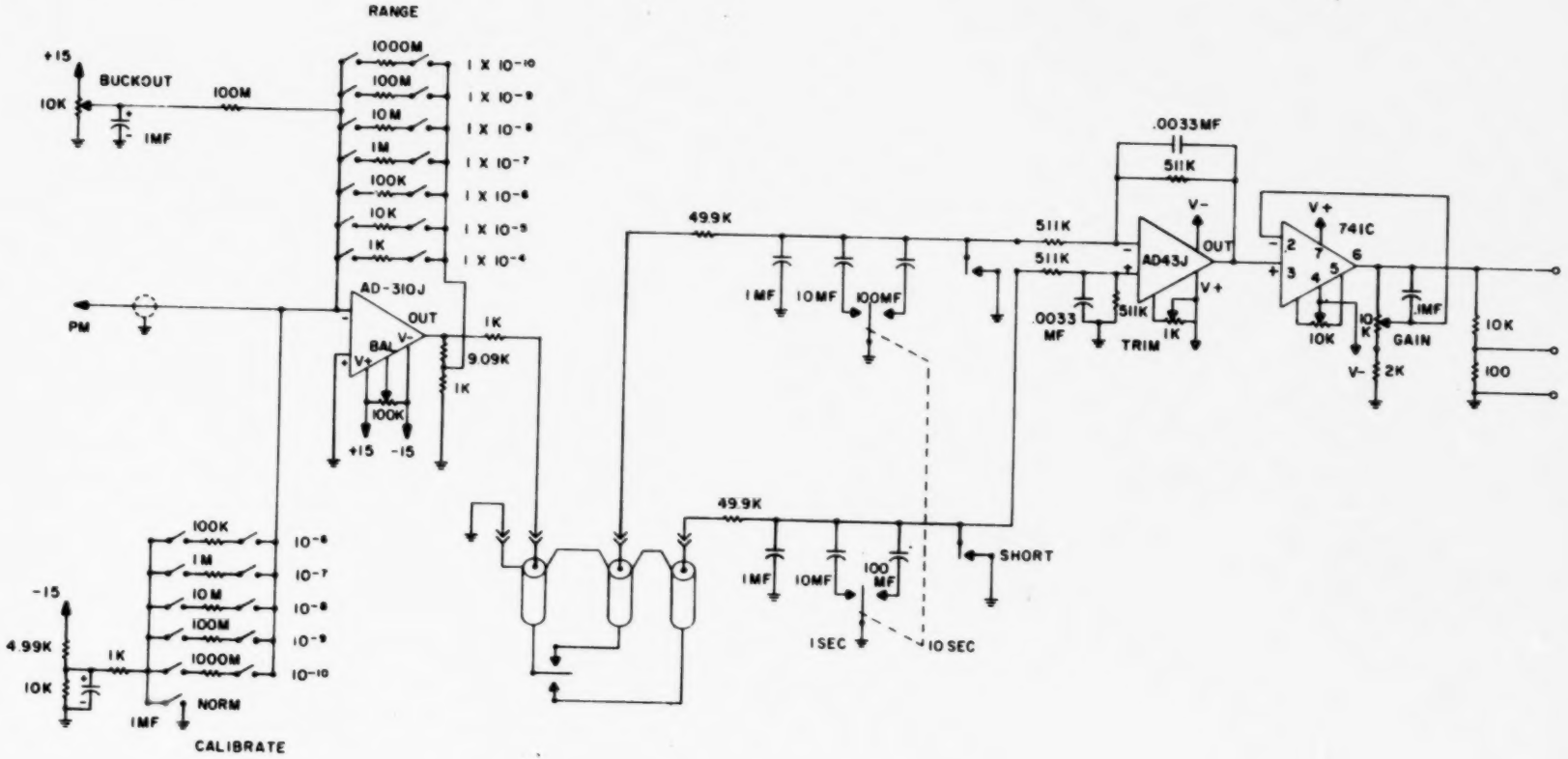

FIGURE 10. AMPLIFIER/DEMODULATOR SCHEMATIC

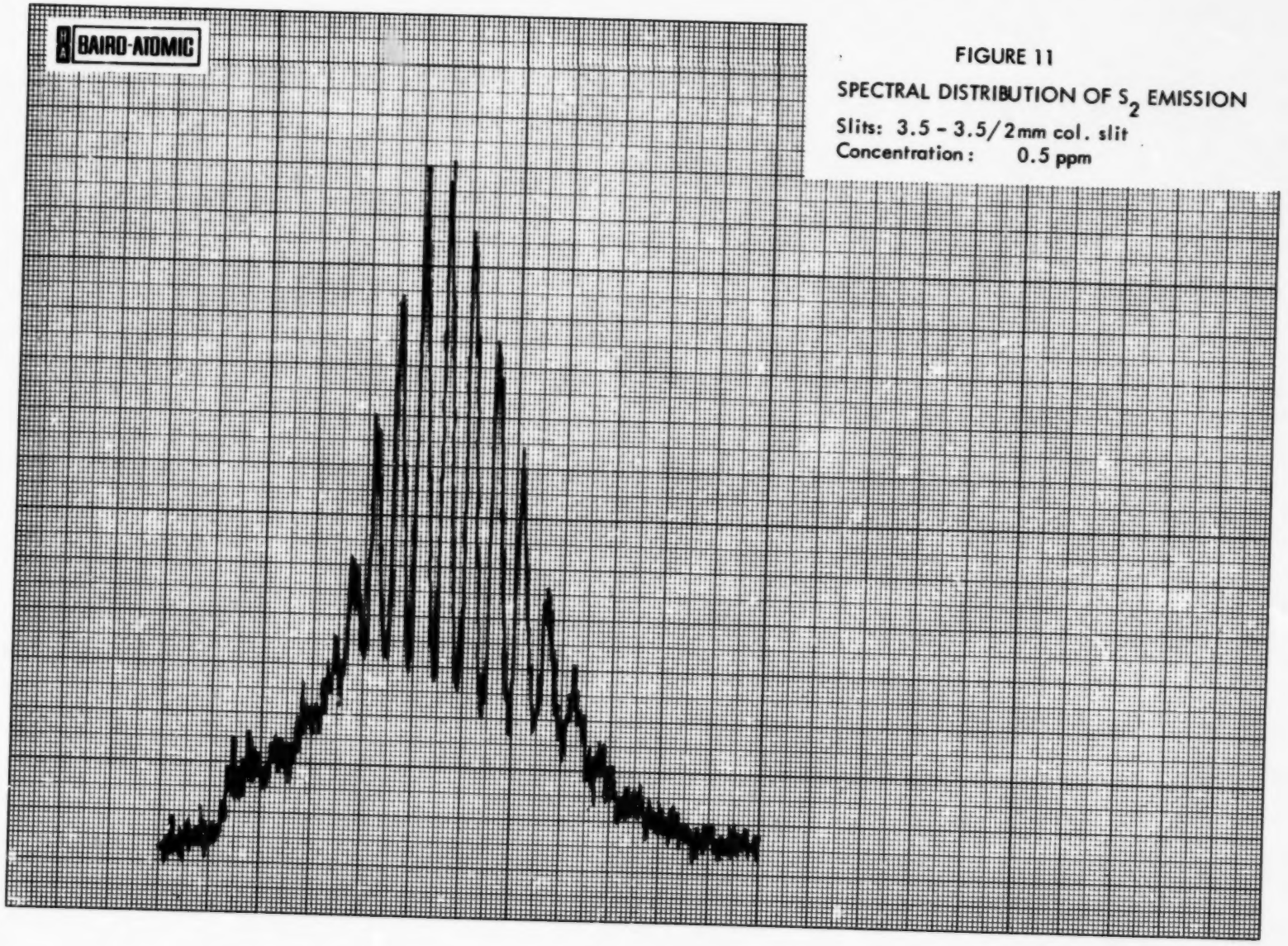

FIGURE 11

SPECTRAL DISTRIBUTION OF S_2 EMISSION

Slits: 3.5 - 3.5/2mm col. slit

Concentration: 0.5 ppm

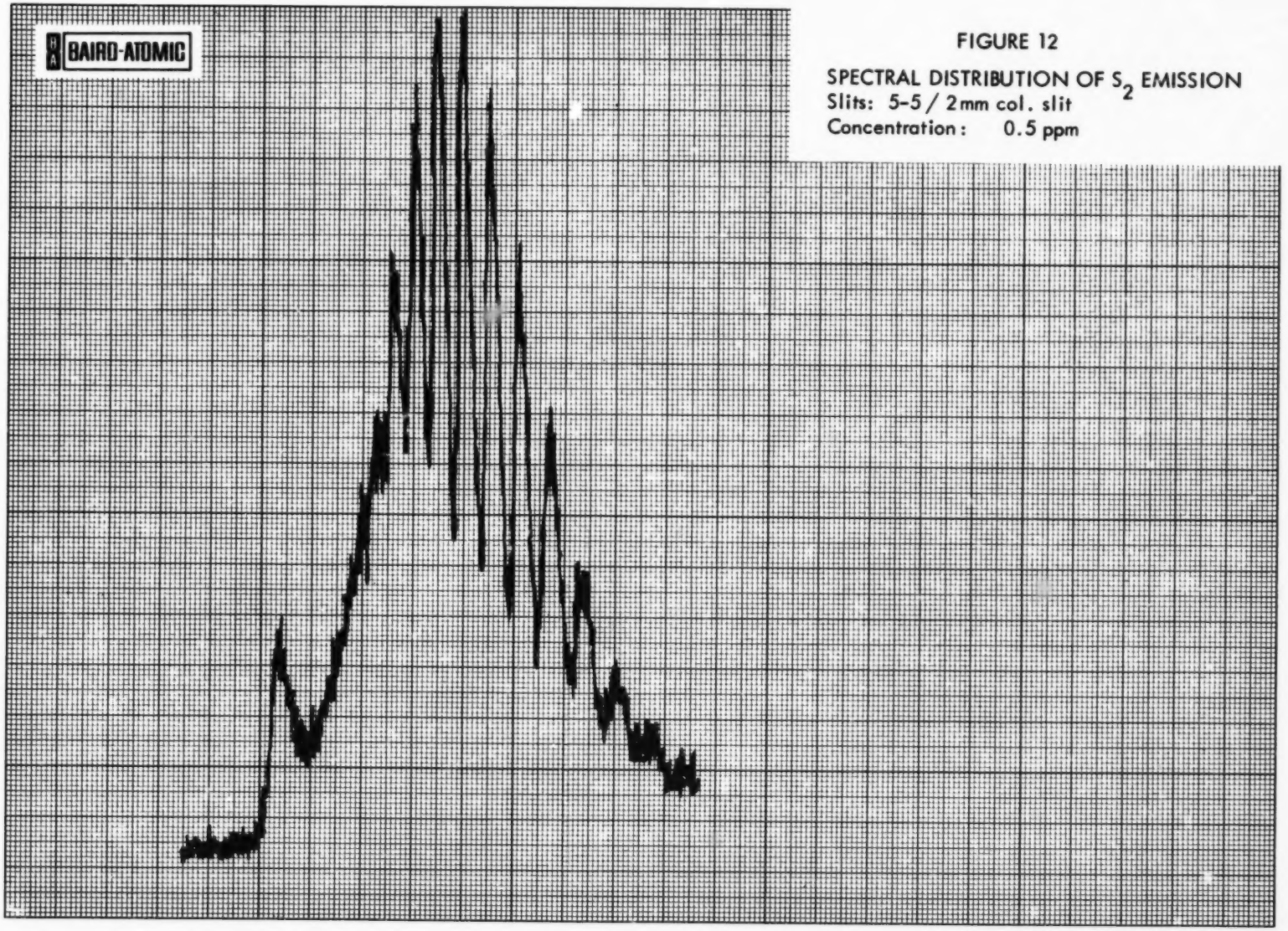

FIGURE 12

SPECTRAL DISTRIBUTION OF S_2 EMISSION
Slits: 5-5 / 2mm col. slit
Concentration: 0.5 ppm

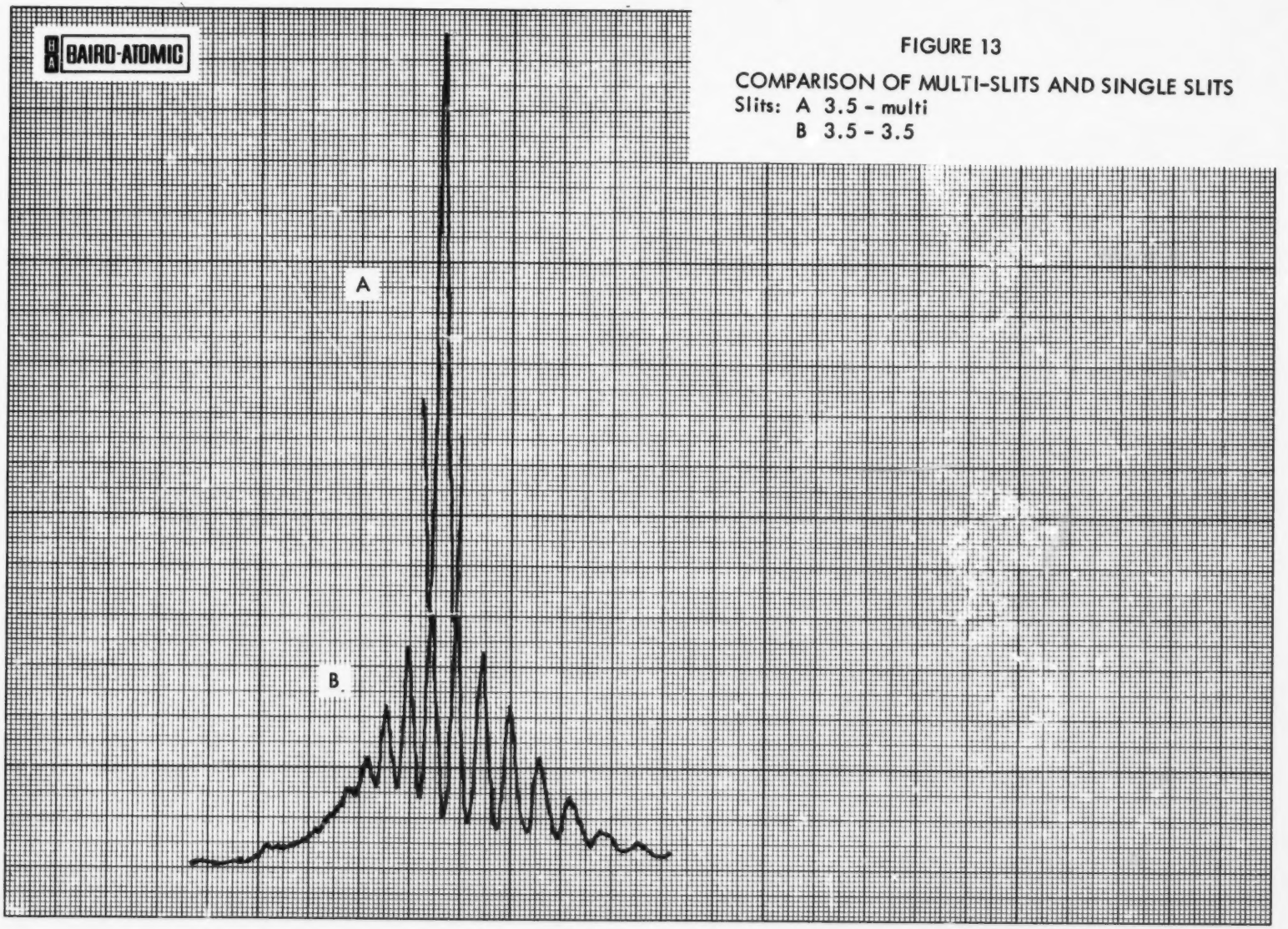

FIGURE 13

COMPARISON OF MULTI-SLITS AND SINGLE SLITS
Slits: A 3.5 - multi
B 3.5 - 3.5

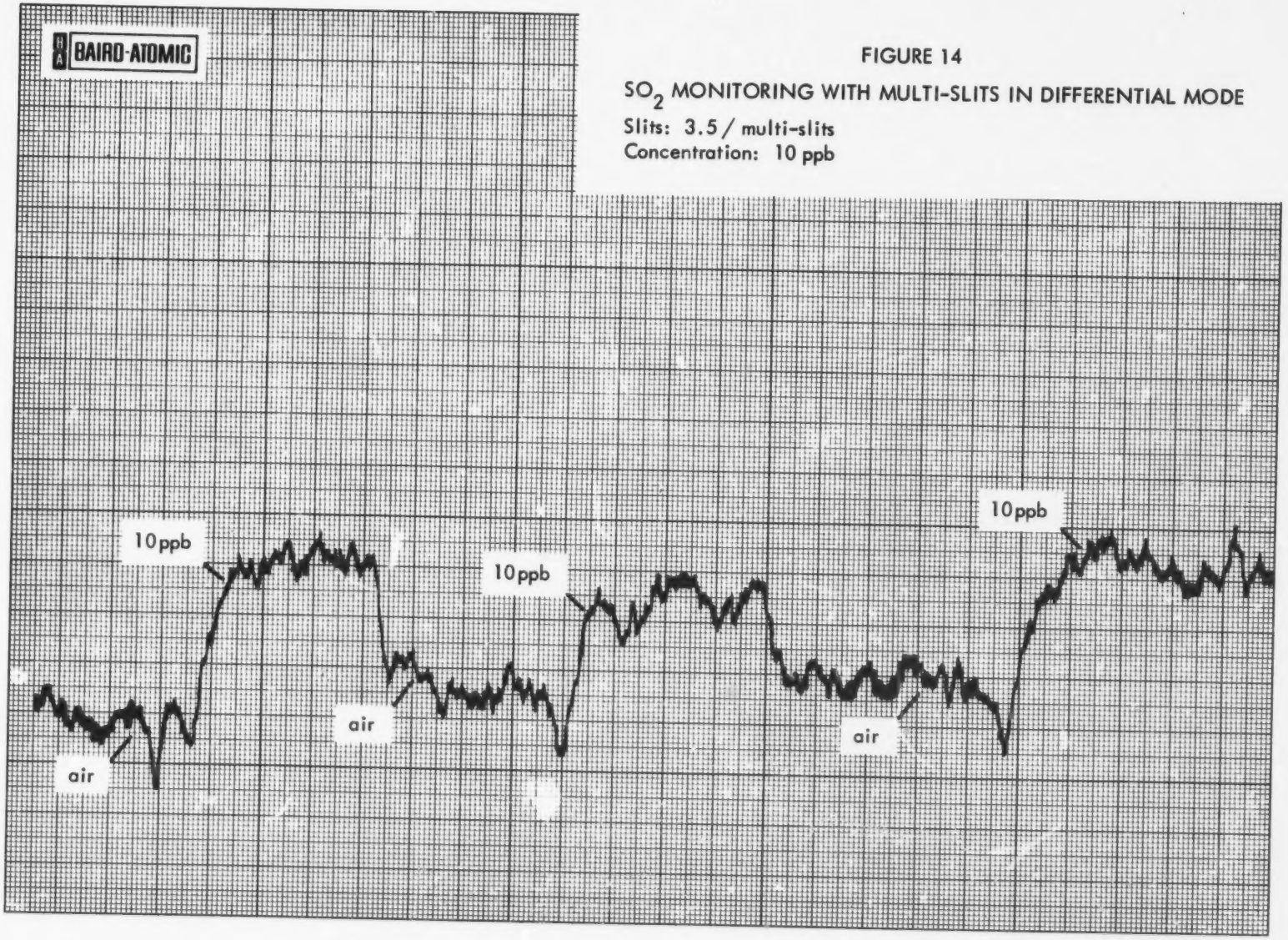

FIGURE 14

SO_2 MONITORING WITH MULTI-SLITS IN DIFFERENTIAL MODE

Slits: 3.5 / multi-slits

Concentration: 10 ppb

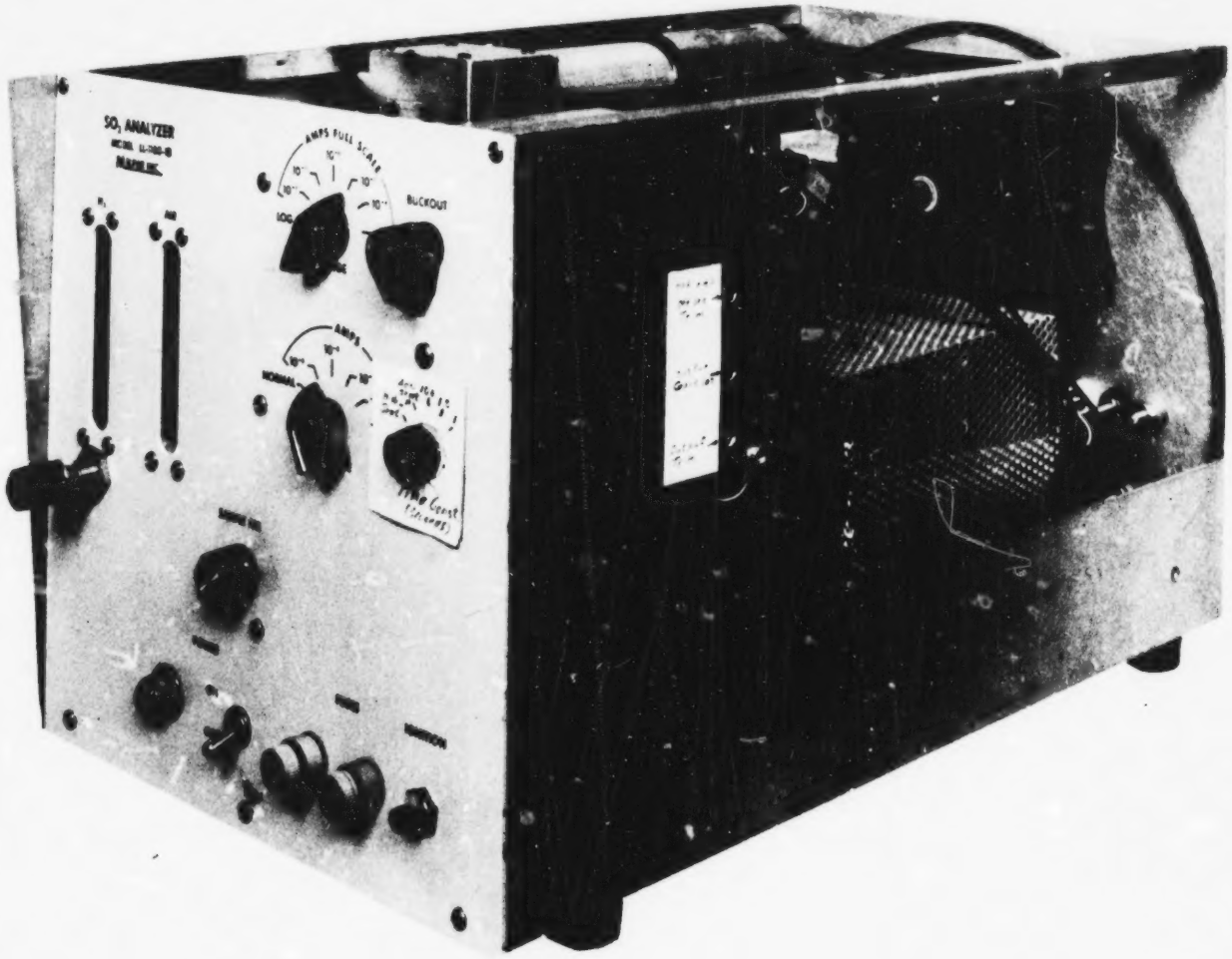

Figure 15. Modified SO_2 Analyzer (Right Side)

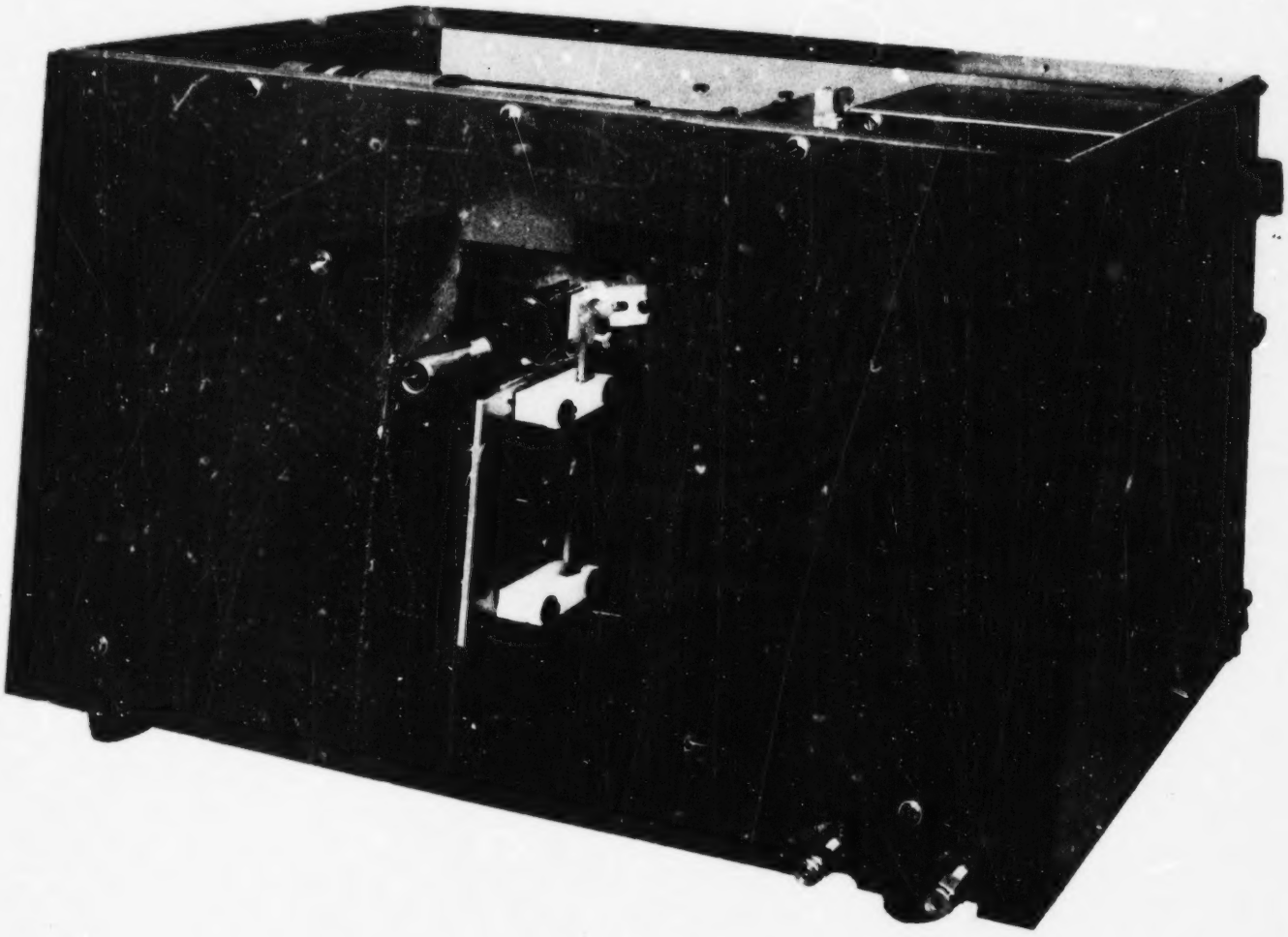

Figure 16. Modified SO_2 Analyzer (Left Side)

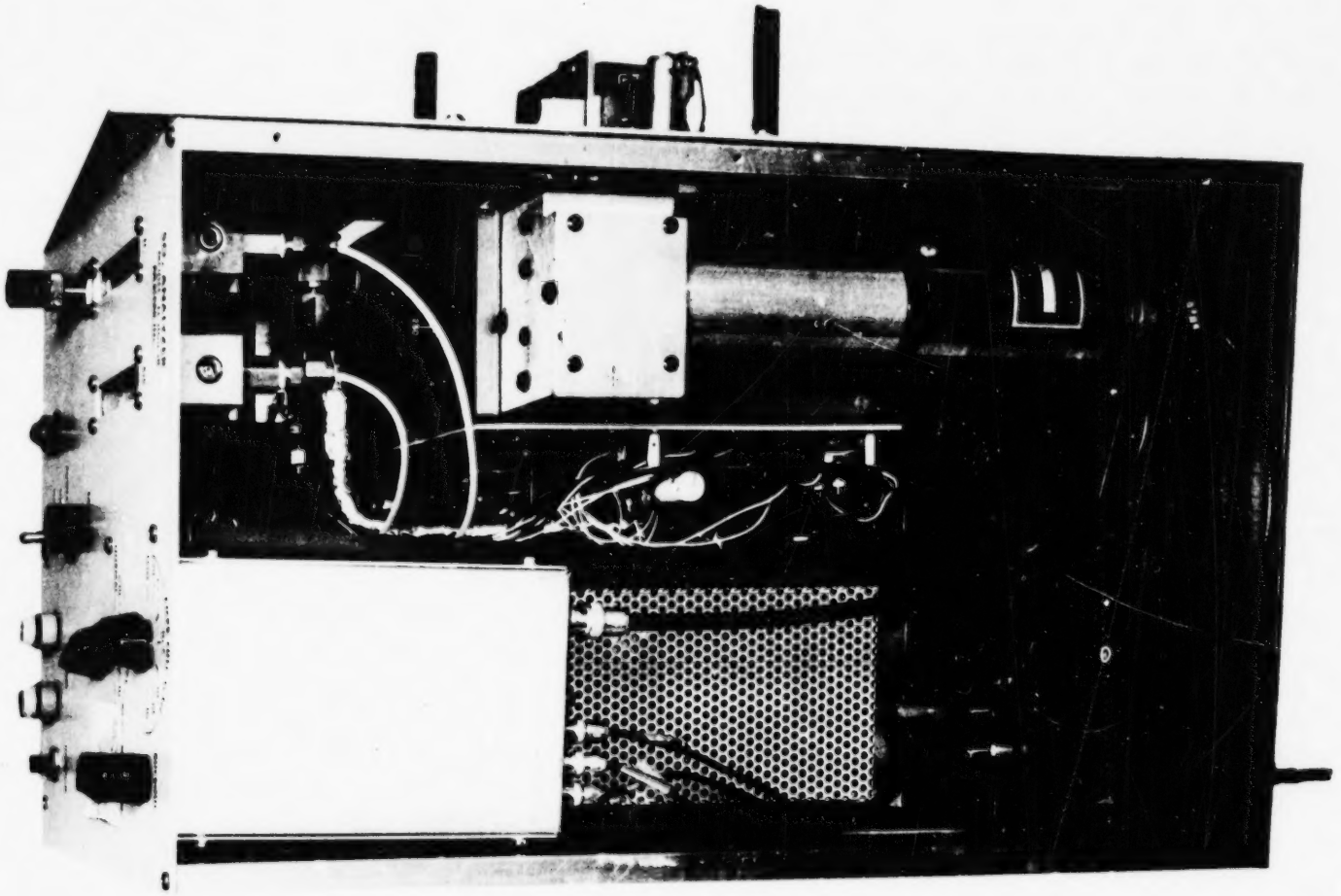

Figure 17. Modified SO_2 Analyzer (Top View)